Investigation of Xanthan Gum Solution Behavior under Shear Flow Using Rheooptical Techniques

Eleanor L. Meyer and Gerald G. Fuller*

Department of Chemical Engineering, Stanford University, Stanford, California 94305

Ross C. Clark

Kelco Division of Merck & Company, Inc., San Diego, California 92138

W.-M. Kulicke

Institut für Technische und Makromolekulare Chemie, Universität Hamburg, Hamburg, F.R.G.

Received July 13, 1992; Revised Manuscript Received October 16, 1992

ABSTRACT: The complementary rheooptical techniques of birefringence and dichroism are used to investigate the dynamics of xanthan gum in dilute/semidilute solution. Because xanthan self-aggregates, there are a range of very different length scales of molecules in solution which the optical methods probe. Birefringence results give information about segmental orientation in flow while scattering dichroism allows interrogation of the much larger aggregate orientation. Two xanthan samples are studied and the results are compared with previous studies. Birefringence and dichroism measurements show very different orientational and relaxational responses in shear flow, indicative of the differences between the structures examined by the two techniques. Dichroism steady-state orientation angle and birefringence/dichroism relaxation results also indicate a critical concentration at approximately 2000 ppm which coincides with that found in the literature by several other investigators and explained by some to be a critical concentration of aggregation. Dichroism measurements detect the presence of aggregates though at concentrations as low as 50 ppm, far below this critical concentration. Overshoots in dichroism, birefringence, and stress signals at approximately 2 strain units are also discussed in light of this aggregation phenomenon. The addition of salt was found to greatly enhance the dichroism signal, providing further evidence that the dichroism signal monitors aggregate dynamics.

1.0. Introduction

The relationship between the structures of water-soluble polymers in solution and their flow properties is of interest in many applications. Increased understanding of how polymer structure contributes to flow dynamics allows better prediction of behavior in many flow situations encountered in industrial applications as in drag reduction[1,2] or enhanced oil recovery.[3] This study involves the investigation of xanthan gum, a high molecular weight extracellular polysaccharide ($M_w \sim 2 \times 10^6$) produced by the bacterium *Xanthomonas campestris*. Xanthan gum is used extensively in industry as a thickening or stabilizing agent due to its unusual solution properties, the most significant being high viscosity at low shear, shear thinning which recovers rapidly once the shearing force is removed, and high resistance to shear degradation. There is little variation of viscosity with temperature, pH, and salt concentration over a large range, nor does precipitation in the presence of multivalent cations occur.[2,4,5]

In the past 20 years several studies have investigated the conformation of the xanthan molecule in solution as well as the self-aggregation of xanthan. These studies indicate that the molecule has a rodlike conformation but that it still has some degree of flexibility.[6] Electron microscopy studies reveal that extensively filtered xanthan from a fermentation broth with 0.1 M sodium chloride has a weight-average contour length of approximately 1000 nm, but ranges between 50 and 5000 nm.[7] Xanthan is typically quite polydisperse with $M_w/M_n \sim 2.8$.[8] In addition, xanthan gum rheological properties vary with acetate and pyruvate content as has been shown by recent research.[9] At sufficient ionic strength, xanthan undergoes a disorder → order conformational transition from a random coil to a single or double helix.[10] With increased concentration and ionic strength, an intermolecular ordering or self-aggregation through hydrogen bonding and entanglement effects becomes increasingly significant. This aggregation phenomenon has been the subject of a great deal of research in the field due to its important influence on the rheological properties of the solution. Many studies have reported a critical concentration of aggregation (c^{**}) of xanthan different from the critical overlap concentration (c^*).

Using mechanical measurements, Rochefort and Middleman[2] observed increases in the ratio of the storage modulus to the loss modulus, $G'(\omega)/G''(\omega)$, and in the magnitudes of the moduli themselves upon the addition of salt to xanthan gum solutions with concentrations above 2000 ppm. Moduli were also found to be less frequency dependent in this concentration range. Below 2000 ppm though, samples exhibited typical semidilute and polyelectrolyte behavior. A strong frequency dependence of the moduli was found over the entire range for samples both with and without salt. The addition of salt was also found to drop the moduli by approximately 75%, a typical polyelectrolyte behavior. When salt is present at these lower concentrations, charge screening causes a collapse of the side chains and an alignment with the backbone which is stabilized by intramolecular noncovalent bonding.[4] Such a transition results in a decrease in the overall hydrodynamic size of the xanthan chain and, thus, a decrease in the solution properties. However, an increase in solution properties, as was seen for concentrations above 2000 ppm, is indicative of increased structure and was argued to be a result of increased aggregation at this concentration level.

Cuvelier and Launay[11] found similar results in their study of xanthan in 0.1 M sodium chloride solution. Also using mechanical measurements, they determined two critical concentrations, $c^* = 280$ ppm and $c^{**} = 1100$ ppm, corresponding to three regions of flow behavior, a dilute

0024-9297/93/2226-0504$04.00/0 © 1993 American Chemical Society

region, an intermediate region, and a semidilute region. The critical concentrations marking the divisions of these regions were found by examining the concentration dependence of the first Newtonian viscosity and by observing the frequency dependence of the complex moduli in viscoelastic experiments. Marked changes in the viscosity versus concentration relationship and reduced frequency dependence of G' and G'' above c^{**} indicated increased structure with increased concentration. They concluded that, at c^*, the onset of molecular overlap occurs, while, at c^{**}, a nonpermanent network is formed through intermolecular associations.

Even when researchers have attempted to eliminate intermolecular associations, as in the study done by Milas et al.,[12] two critical concentrations were still found. In their mechanical measurements of xanthan in 0.1 M sodium chloride, critical concentrations were found to be $c^* = 126$ ppm and $c^{**} = 780$ ppm. Their results are somewhat different from those of the above researchers in that they saw no change in the frequency dependence of the dynamic moduli with increased concentration up to 3000 ppm. Critical concentrations were instead determined from changes in the dependence of the specific viscosity on the overlap parameter $c[\eta]$. It was concluded that c^{**} marks a transition from the semidilute regime to a concentrated regime in which there exists a uniform distribution of polymer segments. The structure in solution for concentrations below 3000 ppm was thought only to be affected by polymer entanglements and not by hydrodynamic interactions.

Jamieson, Southwick, and Blackwell[13,14] have used quasielastic light scattering to characterize the conformation of xanthan in solution. The light scattering technique has the inherent advantage of the ability to probe concentrations below the sensitivity threshold of mechanical measurements. These researchers determined a transition from dilute to semidilute behavior in the diffusion coefficient at approximately 200 ppm in distilled water and a further transition indicative of cooperative interactions between chains at approximately 700 ppm. In a separate study,[15] these researchers found further evidence for time-dependent aggregation of xanthan at concentrations as low as 80 ppm and with a time constant of formation of several days.

It is important to note in comparing the results of any studies with xanthan gum that discrepancies may be due to different sources of the material, variation in the degree of acetate or pyruvate substitution, or differences and dispersity of the molecular weights. In fact, differences in molecular weight have been attributed to the degree of aggregation of the xanthan by Southwick et al.[14] There are some important similarities which we can find in a comparison of their results. In the discussed studies, although differing in the explanations of the respective results, all report a transition in the conformation of xanthan which occurs in the range of 1000–2000 ppm and is caused by increased structure at the higher concentrations. This transition in conformation is greatly affected by salt content as well as by temperature.[2,4,16-18] In addition to the above suggested explanations for differences in results, the sample preparation and ionic content may also greatly affect the structures which cause this transition in solution properties. From the work of Jamieson et al. it is clear that aggregates may re-form once broken apart, further complicating experimentation and interpretation of results.

In this study we have employed the complementary techniques of birefringence and dichroism optics to probe the dynamics of xanthan in solution subjected to a shear flow. These optical methods have advantages over the aforementioned mechanical and light scattering measurements in that mechanical measurements are limited in their sensitivity while light scattering is restricted to quiescent systems. We have successfully used these techniques to monitor the dynamics of both xanthan segments and single chains as well as the much larger aggregates in the dilute/semidilute concentration range of 50–4500 ppm.

2.0. Experimental Section

2.1. Materials. Two different xanthan gum samples were used in this study. The first sample was obtained from the University of Hamburg, Germany. For convenience, it will be called xanthan-1. The sample was received in solution form but was prepared from a powdered xanthan with a water content of 8.9%. The molecular weight was found by wide-angle light scattering to be 9×10^6. Acetate and pyruvate substitution were 69 and 18 mol %, respectively. The powder was diluted in distilled water to 3010 ppm using a magnetic stirrer and stirring for 24 h. Formaldehyde (0.3%) was added as a preservative. Once received in our laboratory, dilutions were made of the sample with distilled water, yielding seven concentrations in the range of 3010 to 52 ppm. This concentration range covers the semidilute/dilute concentration regime for xanthan and crosses the overlap concentration as well as the aggregation concentration cited in the literature.

The second sample used was a powdered xanthan sample, Keltrol T, obtained from Kelco Co., San Diego, CA. We will refer to it as xanthan-2 in this paper. The sample was diluted to approximately 1000 ppm (correcting for water content ~10%) in distilled water by mixing with a blender at approximately 40-W power for 15 min. Shear rates in the blender were not sufficiently high to cause shear degradation. The sample was then stirred for an additional 24 h with a magnetic stirrer. Care was taken in this sample preparation to minimize microgel (unhydrated xanthan) formation which could lead to larger aggregates in solution.[2] This sample was then dialyzed exhaustively to obtain the sodium form of the xanthan molecule. A 24-h dialysis was first performed against 0.1% ethylenediaminetetraacetic acid (EDTA). This was followed by a 3-day dialysis against distilled water, a 3-day dialysis against 0.1 M sodium chloride solution, and an additional 3-day dialysis against distilled water. The sample was filtered through a 5-μm syringe filter to remove any cellular debris. The stock solution was then concentrated to approximately 4467 ppm using a rotary evaporator. The concentration was determined by evaporating the sample at 105 °C for 24 h and weighing the residual film. Reagent grade sodium chloride was added to obtain a 0.05 M salt solution. Sodium azide (0.02%) was used as a bactericide. Additional dilutions were made of the sample with 0.05 M sodium chloride. Twelve samples were studied in the range of 4467 to 112 ppm. Samples were stored at approximately 0 °C.

2.2. Methods. The molecular dynamics of the xanthan solutions in response to a steady shear was monitored using the complementary techniques of birefringence and dichroism. As mentioned previously, such techniques have advantages over mechanical measurements in their enhanced sensitivity, particularly at low concentrations. Briefly, birefringence ($\Delta n'$) and dichroism ($\Delta n''$) are the anisotropic retardation and the anisotropic attenuation, respectively, of light as it passes through an oriented material. This orientation could be induced by a number of forces such as a flow or an electric field. In this study, orientation is accomplished by a steady-shear flow using a Couette geometry. Light is passed along the vorticity axis, thus allowing sampling of the shear plane and facilitating calculation of the degree of orientation in the shear flow.

Birefringence in the samples of interest here is primarily an intrinsic effect due to anisotropy in the polarizability of the polymer segments. Measure of birefringence therefore gives insight into the local orientation of polymer segments. Because xanthan does not absorb light of the wavelength used in this study (632.8 nm), we do not expect intrinsic dichroism in our

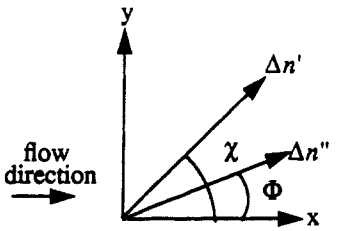

Figure 1. Definitions of the birefringence ($\Delta n'$) and dichroism ($\Delta n''$) orientation angles. Flow is from the left to right.

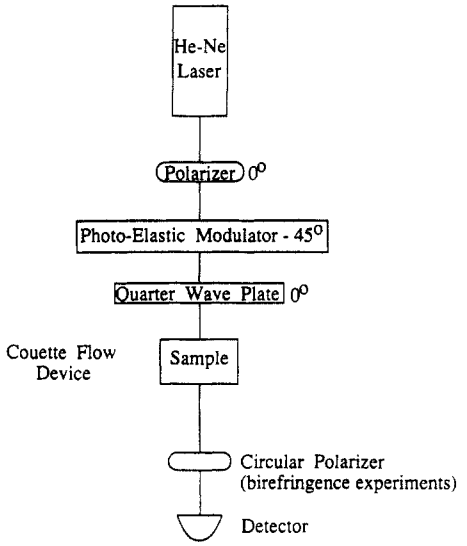

Figure 2. Schematic of the optical train.

experiments. The presence of dichroism is therefore a form or scattering effect caused by the orientation of large particles, in general a much larger length scale than that probed by birefringence. We believe, in the case of xanthan, the resulting signal must be due to aggregates in solution. The two different length scales probed by these techniques may or may not have the same orientation angle with respect to the flow direction. We define the orientation angle measured in birefringence as χ and the orientation angle measured in dichroism as Φ as shown in Figure 1. For further details regarding these techniques we refer the reader to the reference by Fuller.[19]

A schematic of the optical train used in this study is shown in Figure 2. As indicated, a simple removal of the circular polarizer allows one to change the experimental apparatus from one measuring birefringence to one measuring dichroism. The light source is a polarized helium–neon laser of 632.8-nm wavelength. The beam first passes through a 0° polarizer, a photoelastic modulator at 45°, 52-kHz frequency, and a 0° quarter-wave plate. This upper portion of the optical train defines the polarization of the light and provides the modulation of that light necessary for determination of the birefringence and dichroism of the sample. Next the modulated beam enters the sample held in a Couette flow cell, traveling along a path perpendicular to the plane defined by the flow and velocity gradient vectors (path length 1.37 or 2.44 cm). The exiting beam either is passed through a circular polarizer and then collected at the detector in a birefringence experiment or simply collected at the detector in dichroism experiments. The resulting intensity in either case is of the form

$$I = I_{DC} + I_{\omega} \sin(\omega t) + I_{2\omega} \cos(2\omega t) + \ldots$$

where ω is the frequency of the photoelastic modulator and t is time. The use of lock-in amplifiers set at reference frequencies corresponding to ω and 2ω allows one to determine the Fourier coefficients, I_{ω} and $I_{2\omega}$, which are functions of the birefringence or dichroism and the corresponding orientation angle. Further details regarding the mathematical treatment of the experiment can be found in ref 20.

For each concentration, experiments were performed with shear rates ranging from 1 to 50 s^{-1}. The start-up, steady-state, and relaxation behavior were recorded for both birefringence and dichroism experiments. Experiment duration was sample dependent. To properly determine the birefringence or dichroism from I_{ω} and $I_{2\omega}$, the Bessel functions to which these coefficients are proportional must be calculated. This calibration was accomplished by rotating a quarter-wave retarder, the birefringence of which is known, in the sample position and calculating appropriate Bessel function values. All experiments were performed at room temperature, approximately 23 °C. Results presented represent averages of three identical experiments for each given shear rate on each sample concentration.

In addition, stress overshoot measurements were made of the xanthan-1 sample at Lockheed Missiles & Space Co. Inc., Palo Alto, CA. Experiments were performed with a dynamic stress rheometer (Rheometrics Model RMS-800) in a cone-and-plate geometry. The cone was 50 mm in diameter and had a cone angle of 0.04 rad. The measurements were made at room temperature, approximately 23 °C, and performed on concentrations down to the sensitivity limits of the instrument.

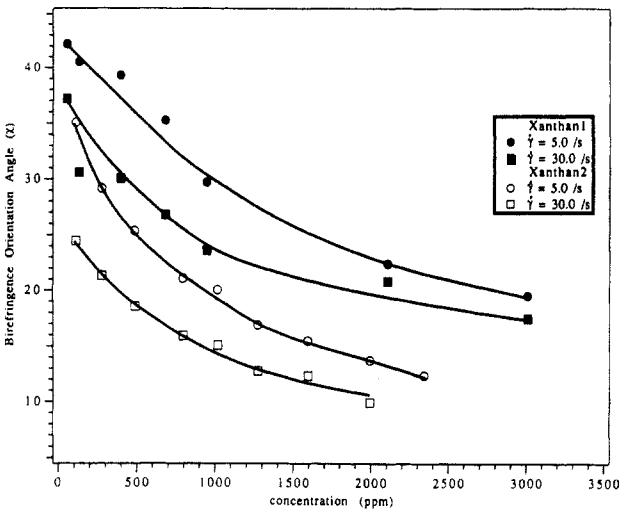

Figure 3. Birefringence steady-state orientation angle (χ) vs concentration of xanthan-1 and xanthan-2 at two shear rates, $\dot{\gamma}$ = 5 and $\dot{\gamma}$ = 30 s^{-1}.

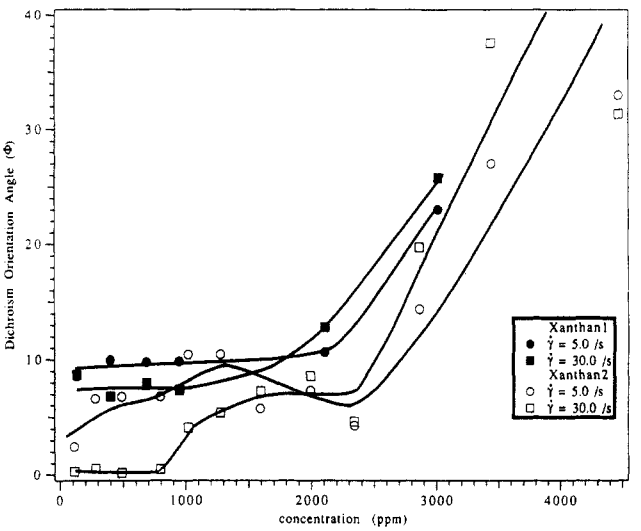

Figure 4. Dichroism steady-state orientation angle (Φ) vs concentration of xanthan-1 and xanthan-2 at two shear rates. A critical concentration regime is indicated by the rapid increase in orientation angles at approximately 2000 ppm.

3.0. Results and Discussion

3.1. Steady-State Behavior. The results of the two optical experiments reveal two very different orientational responses over the semidilute/dilute concentration regimes for both xanthan samples. As shown in Figures 3 and 4, the orientation angles of birefringence and dichroism with

respect to the flow direction differ in magnitude as well as in their dependences on concentration. Alignment in the flow direction is defined to be 0°. The birefringence data in Figure 3 follow the usual result of decreasing orientation angle with increasing concentration. At low concentrations, the orientation angle tends to 45°. This can be explained by the fact that at increasingly higher concentrations, the rotational component of the shear flow field can more easily orient a given molecule in the flow direction due to increased segment/segment interactions. At lower concentrations, Brownian motion tends to counter the rotational component of the flow field, allowing the extensional component to dominate the orientation at 45°.

Data are presented for concentrations of xanthan-2 only up to approximately 2000 ppm. For concentrations above this sample, the birefringence went over multiple orders. Because the signal ratios in the data are both proportional to sin (δ') (where $\delta' = (2\pi\Delta n'd)/\lambda$, δ' = retardation, d = path length, λ = wavelength of incident light), as δ' passes through multiple orders of $\pi/2$, the signals show oscillations in start-up and relaxation. If the steady-state retardation equals π, the resulting signal is greatly influenced by the birefringence of the quartz flow cell windows. The orientation angle cannot be accurately calculated when this occurs and shows discontinuities in its dependence on concentration and shear rate. Although the "over orders" phenomenon does not affect the dichroism calculation in this case and the birefringence can be extrapolated, unfortunately this phenomenon prevents calculation of the birefringence orientation angle. Such discontinuities in the orientation angle when the birefringence goes through multiple orders are discussed further in the text by Janeschitz-Kriegl.[21]

The dichroism angle shown in Figure 4 indicates a very different and unexpected steady-state behavior. Unlike the birefringence, dichroism orientation angles are low (in the flow direction) for low concentrations, but beyond a critical concentration in the range of 2000 ppm rise rapidly. If the two optical techniques both examined single-chain effects, we would see similar orientation angle behavior in the birefringence and dichroism experiments. Instead birefringence and dichroism orientation angles have almost opposite concentration dependences, indicating dichroism must be monitoring a different orientational response. Because dichroism is sensitive to longer length scales than birefringence and xanthan gum is known to self-aggregate, one is led to conclude that the presence of dichroism indicates the existence of aggregates. Furthermore, as Figure 4 illustrates, we are able to detect dichroism at the very lowest concentrations studied, far below the critical concentration of aggregation (c^{**}) cited in the literature.

Our observation of aggregates in solutions of concentrations as low as 50 ppm is supported by the study by Southwick et al. using quasielastic light scattering. These researchers describe a time-dependent aggregation effect at concentrations down to 80 ppm, even for samples which had been previously filtered to remove aggregates. Other than the care used to fully hydrate the powdered xanthan, additional procedures such as extensive filtration to eliminate aggregation were not made. It is therefore not surprising in light of the Jamieson group work that we find aggregates at very dilute concentrations. The high molecular weight reported for xanthan-1 by the Kulicke group also indicates that the presence of aggregates is likely. Discrepancies in molecular weight reports have been attributed by Southwick et al. to differences in the degree of aggregation.[15] It is most likely that molecules at the lowest concentrations are joined through hydrogen-

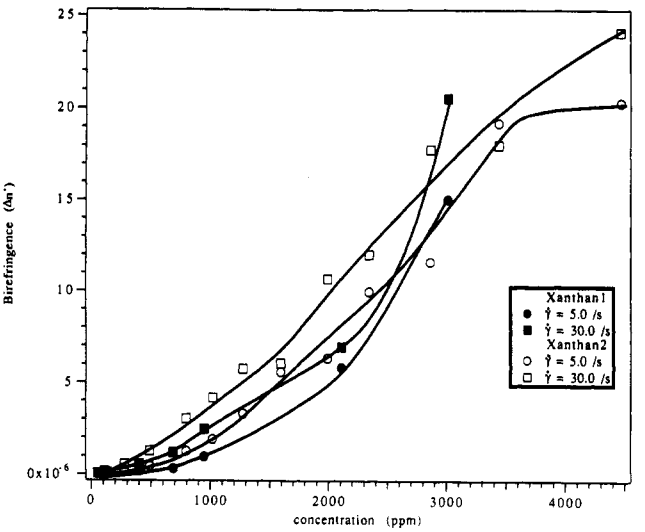

Figure 5. Concentration dependence of steady-state birefringence of xanthan-1 and xanthan-2 at two shear rates.

bonding and ionic effects rather than through entanglements since the probability of molecular overlap is so low there.

Interestingly, the range in concentration in which the rapid increase in angle occurs seems to coincide with the c^{**} cited in the literature (approximately 2000 ppm), indicating that, indeed, a very different flow behavior occurs in this concentration range. The coincidence of the position of the sudden change in orientational behavior for xanthan-1 and xanthan-2 and with the c^{**} found by Rochefort and Middleman in particular[2] is encouraging and leads us to believe this phenomenon may be general for xanthan with similar preparation techniques.

The differences in the orientational behavior of the aggregates and segments or free chains is puzzling. It appears that at high concentrations (above c^{**}), the presence of these large aggregates prevents alignment in the flow direction while free chains and/or the segments making up the aggregates are more easily aligned in the flow direction. Below c^{**}, single chains are oriented at higher angles as expected, but aggregates are oriented with the flow. Perhaps this can be explained by the "weak-gel networking" described in the literature at high concentrations.[2,22,23] Above c^{**}, increased intermolecular entanglements and hydrogen bonding may form a complicated structure which resists alignment in the flow, while below c^{**} many of these entanglements may be gone, leaving only dispersed aggregates. Due to their larger size, these dispersed aggregates may then be more easily oriented in the flow than the free chains of the solution.

The magnitudes of the steady-state birefringence and dichroism at shear rates of 5 and 30 s^{-1} for xanthan-1 and xanthan-2 are shown in Figures 5–7. A steady increase in each optical anisotropy with concentration is seen. Unlike the orientation angle behavior, there is no indication of a critical phenomenon in any of these data. The steady-state birefringence data shown in Figure 5 show similar behavior for xanthan-1 and xanthan-2. The agreement between the magnitudes of the birefringence indicates comparable anisotropies in the orientation of segmental and single-chain xanthan in both samples.

Previous electric birefringence studies performed by Besio et al.[24] and Morris et al.[25] have shown that the birefringence of native xanthan is greater than that of renatured or denatured (disordered) xanthan, although birefringence values lie within the same order of magnitude. The addition of salt to the xanthan-2 solution should

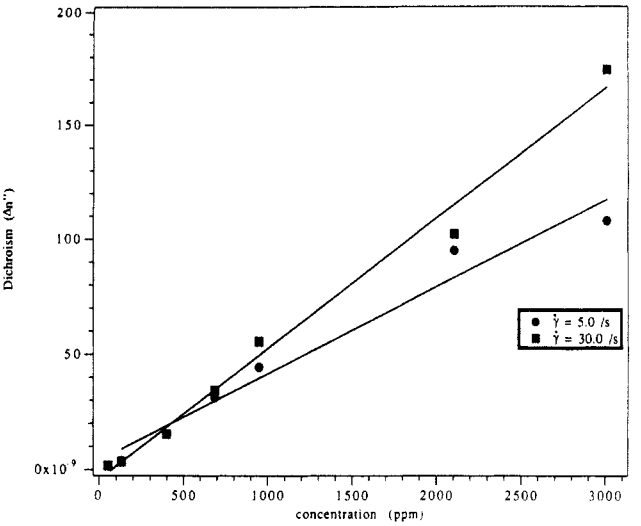

Figure 6. Concentration dependence of steady-state dichroism of xanthan-1 at two shear rates.

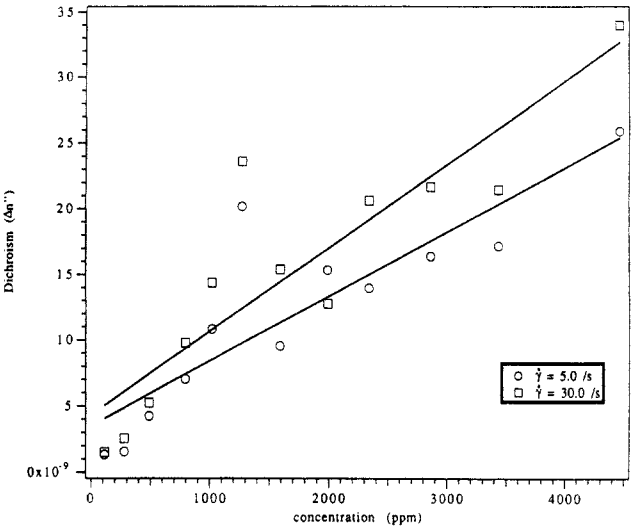

Figure 7. Concentration dependence of steady-state dichroism of xanthan-2 at two shear rates. Although the magnitude of the dichroism is significantly lower than that shown in Figure 6, a similar qualitative behavior is seen.

ensure that the molecule is predominantly in the ordered state but it is difficult to assess what the exact conformation of xanthan-1 might be. The small differences between the steady-state birefringences of the two samples might be attributed in part to differences in degrees of ordering, but because of the many experimental variables involved, we suggest that this is only one of many possible explanations. Furthermore, it has also been shown that regions of disorder and order can coexist in solution and even on the same molecule.[7,26] Similarities between the birefringences of the two samples would indicate that xanthan-1 has at least some molecular ordering, particularly in light of the dichroism data. The presence of aggregates at concentrations as low as 50 ppm would indicate that some degree of molecular ordering exists there.

Steady-state dichroism for xanthan-1 and xanthan-2 in Figures 6 and 7 show an almost linear dependence of dichroism on concentration. These results again support the hypothesis that we are probing aggregate dynamics with this technique. One will notice that in Figure 6, the magnitude of the steady-state dichroism covers 2 orders of magnitude over the concentration range while in Figure 7, only 1 order of magnitude is covered. Additional work with xanthan-2 indicates that the dialysis treatment and the filtration of the sample do not affect the magnitude

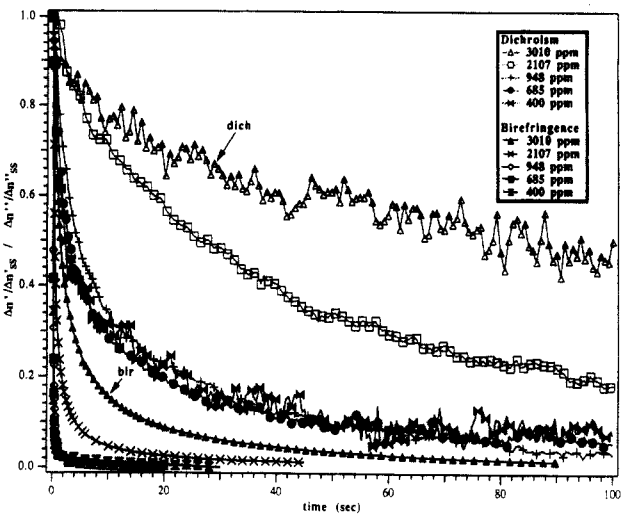

Figure 8. Normalized birefringence/dichroism relaxation subsequent to the cessation of steady shear at time = 0 s, $\dot{\gamma} = 30\ s^{-1}$. Various concentrations of xanthan-1 are presented. Data are normalized by the corresponding steady-state birefringence/dichroism. The overlap of curves below c = 2107 ppm may indicate the existence of a critical concentration in this regime.

of the dichroism of this sample significantly. It is therefore unlikely that the ionic content of the sample could affect the dichroism to this degree. The viscosities of the two xanthan samples are also comparable in magnitude.

Differences between the dichroism of these samples may be due to a number of other factors. First of all, because solutions of the two powdered samples were prepared differently (stir bar versus blender), it is possible that xanthan-1 was not as well hydrated in preparation as in the case of xanthan-2. Poor hydration results in the formation of microgels and can contribute to larger aggregate structures in solution. These larger aggregates may contribute to an increased dichroism signal. There were also certainly some inherent differences in the molecules themselves such as molecular weight, side chain substitution, etc., but it is unlikely that such differences would have such a marked effect.

The xanthan-1 solution also appeared more cloudy than the xanthan-2 solution, even prior to filtration of the xanthan-2 solution. Such an appearance is usually attributed to cellular debris. The xanthan-2 sample had been extensively treated to remove cellular debris for commercial applications, even prior to our dialysis and filtration. In fact, the additional filtration of the xanthan-2 sample through the 5-μm filter had no effect on the magnitude of the dichroism in this sample. The many similarities between the orientational behaviors of the two samples indicate that the presence of cellular debris does not affect the qualitative behavior in the dichroism experiment and thus, we do not feel the dichroism signal is due to cellular debris in solution. It is possible however that the attachment of cellular debris to xanthan aggregates or microgels may result in a substantially larger structure in solution which causes the large dichroism signal.

3.2. Transient Behavior. 3.2.1. Relaxation. The existence of a critical concentration also appears to be present in birefringence/dichroism relaxation for xanthan-1 as shown in Figure 8. It is obvious from the plot that dichroism relaxes over a much longer time scale than the birefringence. Relaxation of the dichroism continues beyond the scale of the figure for an additional 100–200 s. This is an expected result since larger particles have a longer relaxation time than smaller ones. Again this

difference in relaxation times indicates the two different phenomena that these complementary techniques probe at all concentrations studied. The overlap of the normalized relaxation curves of both dichroism and birefringence also indicates the presence of a critical concentration in the range of 1000–2000 ppm, just as seen in the dichroism orientation angle and in the literature. Additional shear rates other than 30 s^{-1} show similar, although not as dramatic, behavior.

It should be noted that this critical concentration phenomenon in the relaxation dynamics is not as apparent in the xanthan-2 sample. Although the birefringence dynamics and curve overlaps indicate that a critical concentration may exist in the 2000 ppm range, the dichroism normalized curves are scattered and do not show the effect seen in xanthan-1. It is possible that had more samples been taken in the range of 1000–2000 ppm, the effect would not be as pronounced.

Upon analysis, double-exponential curve fits were found to reasonably describe both birefringence and dichroism relaxation data. In most cases the fast mode of the dichroism experiment is of the same order of magnitude as the slow mode of the corresponding birefringence experiment. For example, τ_s(birefringence) = 2.98 s while τ_f(dichroism) = 3.29 s and τ_s(dichroism) = 32.04 s for the concentration of c = 948 ppm pictured in Figure 8. This agreement could be explained by the fact that molecular orientation also contributes to the dichroism signal provided the length scale of that orientation is of the order of the wavelength of the light source. The helical rodlike conformation of xanthan would further increase this molecular orientation as observed in birefringence studies of polymer molecules. Since the normalized birefringence curves collapse below 948 ppm, there does not appear to be any apparent disorder/order transition with concentration unless it too occurs in the c^{**} region.

Because the dichroism experiment probes longer length scales though, it will be more sensitive to aggregates than single chains. The slower dichroism time scale is probably a consequence of the aggregate relaxation. Slower relaxation modes in quasielastic light scattering have also been attributed to the presence of aggregates in previous studies.[14] Due to the substantial polydispersity as well as varying degrees of aggregation of xanthan in general, there are of course multiple length scales which contribute to the different modes of relaxation of the polymer in solution. The relative importance of each time constant in the dichroism signal will be weighted according to its concentration in solution. The substantially longer relaxation mode of the dichroism signal coupled with the strong evidence of aggregation in xanthan leads us to believe that the aggregates are the principal contributors to this scattering phenomenon.

3.2.2. Signal Overshoot. As mentioned in the Methods section, start-up experiments were also performed. In these experiments, we examined the overshoot of signals upon inception of shear. Both xanthan-1 and xanthan-2 showed a large overshoot at approximately 2 strain units. An example of this phenomenon is shown in Figure 9 for 2107 ppm. This overshoot was present at all shear rates studied in the range of 1–100 s^{-1} and in all concentrations studied. The signal of interest here in the dichroism is proportional to sin $(2\Phi)\delta''$ (where $\delta'' = (2\pi\Delta n'' d)/\lambda$). Thus an overshoot indicates a rapid increase and decrease in the orientation angle of the aggregates. Similarly, in the birefringence experiment, the signal related to sin (2χ) sin (δ') also shows an overshoot at 2 strain units. The overshoots are present in calculation of the birefringence

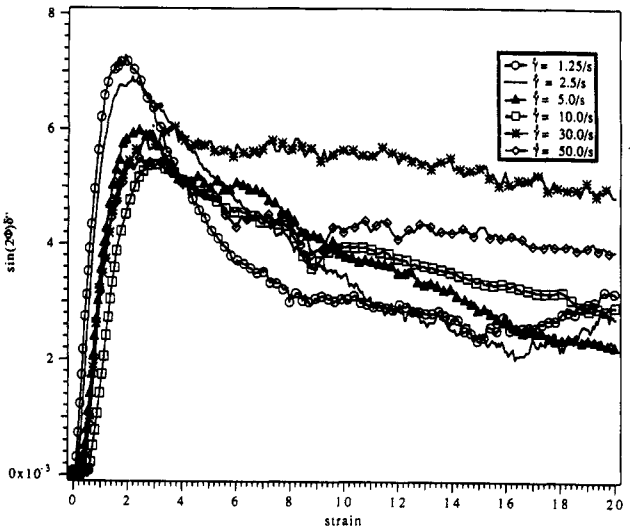

Figure 9. Start-up dichroism signal dependence on strain for various shear rates. Data are presented for 2107 ppm xanthan-1. The overshoot maximum occurs in the range of 2–3 strain units in all experiments.

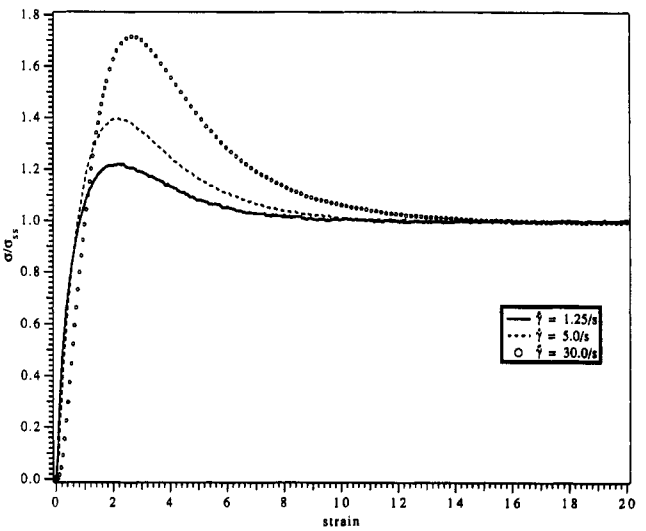

Figure 10. Normalized stress overshoot upon start-up of steady shear vs strain units. Data are presented for 2107 ppm xanthan-1 at three different shear rates. Again, the peak maximum lies in the range of 2–3 strain units.

and dichroism but are less dramatic than the signals proportional to sin (2θ), where θ is the orientation angle.

Chow and Fuller also investigated the birefringence overshoot of a 300 ppm xanthan sample in a 90% glycerin and 10% water solution.[27] They examined birefringence overshoots for shear rates between 10 and 100 s^{-1}. Overshoots in this study appear to also be in the range of 2 strain units. In investigating the effects of salt on conformation, they saw up to a 20% increase in the normalized birefringence overshoot with the addition of sodium chloride (0.1 M) at a shear rate of 92 s^{-1}, with the magnitude of this difference decreasing with decreasing shear rate. This increase was attributed to an increased stiffening of the molecule with the addition of salt.

To investigate this overshoot phenomenon further, stress start-up experiments were performed with xanthan-1 sample. Although concentrations below 400 ppm could not be studied due to the sensitivity limitations of the mechanical techniques, a similar overshoot at 2–3 strain units was seen for those concentrations studied. Data for 2107 ppm are presented in Figure 10 for three shear rates. Although the magnitude of the stress overshoot increases with increasing shear rate, there is no such general trend

in the dichroism signal data which is true for all concentrations studied.

Rochefort and Middleman studied the reassociation of xanthan after shearing by examining the stress overshoot at different times after a high preshear ($\dot{\gamma}$ = 100 s^{-1}).[28] Using their data for 5000 ppm xanthan in distilled water and 0.5% salt solution, $\dot{\gamma}$ = 10 s^{-1}, we calculate similar overshoot behavior with a peak overshoot value in the range of 2–3 strain units independent of reassociation time.

The similar scaling between the birefringence, dichroism, and stress overshoots with strain possibly indicates the contribution of the aggregate structures as well as the single chains to the overall stress of the solution. It is likely that the relative importance of each structure to the stress is largely a function of both concentration and shear rate. Additional experiments are being planned to investigate this relationship.

3.3. Salt Effects. As indicated in the Introduction, many researchers have studied the effects of salt on xanthan conformation and the solution rheology. An increase in salt concentration is thought to enhance the intermolecular attractions between neighboring xanthan chains, thus causing increased aggregation. Dichroism results in this study show additional evidence of this effect. In the xanthan-2 sample, some optical measurements were performed on the dialyzed sample prior to the addition of salt. Following dialysis with distilled water, a 0.1 M sodium chloride solution, and additional dialysis against distilled water, the xanthan molecules should be in the sodium form; that is, the side chain substitution should be Na^+, but excess ions in solution should be minimal. Many studies of xanthan in distilled water indicate that it is highly extended and disordered in conformation. Although aggregation may occur through entanglements at high concentrations, intermolecular attractions through ionic effects are minimized. It is not until salt is added at sufficient concentrations that xanthan can become helical in conformation, undergoing a disorder/order transition, and therefore assume a more rodlike form. Furthermore, the addition of salt is necessary for sufficient attractions to occur to cause aggregate formation.

In the study of xanthan-2 in distilled water, the magnitude of the dichroism signal was substantially diminished and the signal to noise ratio was quite high. Relaxation times were much faster than for the xanthan-1 solution and xanthan-2 in 0.05 M NaCl and lacked the slow mode due to aggregates mentioned in section 3.2.1. This would indicate that the strength of intermolecular interactions was significantly lessened and perhaps also that the xanthan molecules were not in the ordered, helical conformation which would contribute to the overall magnitude of the dichroism signal. Even more interesting, the overshoot in the dichroism signal was completely absent although that of the birefringence experiment was still present. This difference in the dichroism results for the sample with and without salt again lends credibility to the claim that we monitor aggregate orientation with the dichroism signal. Although it appeared that some aggregation was present in the distilled water solution, it seemed to be substantially lower than in the samples studied previously. Because no dialysis was performed on the xanthan-1 sample, there is little insight into the degree of aggregation of this sample, making comparisons to xanthan-2 difficult. Although we are unable at this time to fully explain the overshoot behavior in the dichroism and its parallel with that of birefringence and dichroism, its appearance with increased aggregation leads us to believe that it is linked to this intermolecular networking of the xanthan chains.

4.0. Conclusions

We have successfully used the optical techniques of birefringence and scattering dichroism to monitor xanthan gum single-chain and aggregate dynamics in shear flow. Unlike the mechanical and light scattering techniques employed previously, dichroism allows us to directly probe the aggregate orientational behavior. Evidence of this was found in the very different orientational as well as relaxation behaviors in the dichroism and birefringence experiments. Furthermore, the addition of salt was found to greatly enhance the magnitude of the dichroism signal, providing further proof that dichroism monitors aggregates in solution since salt is known to increase the aggregation effect. A critical concentration was found to be present in the range of 2000 ppm for both xanthan samples studied. The critical concentration is consistent with the critical concentration of aggregation c^{**} found by many researchers in the literature, but unlike several of these studies, we found xanthan aggregates present in all solutions ranging from 50 to 4500 ppm, far below c^{**}. Such findings are consistent with studies done by Jamieson et al., who observed aggregates forming at concentrations as low as 80 ppm. The presence of overshoot in both birefringence and dichroism signals as well as in the stress at approximately 2 strain units indicates that both single chains and aggregates may be important in contributing to the overall stress of the system.

Acknowledgment. We thank A. Chow and C. Ylitalo of Lockheed Missiles & Space Co. Inc. for use of the rheometer and help with the stress measurements of xanthan-1. Polymer samples (xanthan-2) and financial support of this study were provided by the Kelco Division of Merck & Co. Inc. In addition, we gratefully acknowledge the National Science Foundation for graduate fellowship support of E.L.M.

References and Notes

(1) Kulicke, W.-M.; Grager, H.; Kotter, M. *Adv. Polym. Sci.* **1989**, *89*, 1.
(2) Rochefort, W. E.; Middleman, S. *J. Rheol.* **1987**, *31*, 337.
(3) Kulicke, W.-M.; Bose, N.; Bouldin, M. In *Water Soluble Polymers for Petroleum Recovery*; Schulz, D. N., Stahl, G. A., Eds.; Plenum: New York, 1988; pp 1–17.
(4) Morris, E. R. In *Extracellular Microbial Polysaccharides*; Sandford, P., Laskin, A., Eds.; ACS Symposium Series 45; American Chemical Society: Washington, DC, 1977; pp 81–89.
(5) Southwick, J. G.; Jamieson, A. M.; Blackwell, J. *Carbohydr. Res.* **1982**, *99*, 117.
(6) Whitcomb, P. J.; Macosko, C. W. *J. Rheol.* **1978**, *22*, 493.
(7) Stokke, B. T.; Smidsrod, O.; Elgsaeter, A. *Biopolymers* **1989**, *28*, 617.
(8) Holzarth, G. *Carbohydr. Res.* **1978**, *66*, 173.
(9) Kulicke, W.-M.; Oertel, R.; Otto, M.; Kleinitz, W.; Littmann, W. *Erdoel Kohle, Erdgas Petrochem.* **1990**, *43*, 471.
(10) Muller, G.; Anrhourrache, M.; Lecourtier, J.; Chauvateau, G. *Int. J. Biol. Macromol.* **1986**, *8*, 167.
(11) Cuvelier, G.; Launay, B. *Adv. Rheol., Proc. IX Int. Congr. Rheol.* **1984**, *2*, 247.
(12) Milas, M.; Rinaudo, M.; Knipper, M.; Schuppiser, J. L. *Macromolecules* **1990**, *23*, 2506.
(13) Jamieson, A. M.; Southwick, J. G.; Blackwell, J. *J. Polym. Sci., Polym. Phys. Ed.* **1982**, *20*, 1513.
(14) Southwick, J. G.; Jamieson, A. M.; Blackwell, J. *Macromolecules* **1981**, *14*, 1728.
(15) Southwick, J. G.; Lee, H.; Jamieson, A. M.; Blackwell, J. *Carbohydr. Res.* **1980**, *84*, 287.
(16) Holzarth, G. *Biochemistry* **1976**, *15*, 4333.
(17) Jeanes, A.; Pittsley, J. E.; Senti, F. R. *J. Appl. Polym. Sci.* **1961**, *5*, 519.
(18) Milas, M.; Rinaudo, M. *Carbohydr. Res.* **1979**, *76*, 189.

(19) Fuller, G. G. *Annu. Rev. Fluid Mech.* **1990**, *22*, 387.
(20) Johnson, S. J.; Frattini, P. L.; Fuller, G. G. *J. Colloid Interface Sci.* **1985**, *104*, 440.
(21) Janeschitz-Kriegl, H. *Polymer Melt Rheology and Flow Birefringence*; Springer-Verlag: New York, 1983.
(22) Ross-Murphy, S. B.; Morris, V. J.; Morris, E. R. *Faraday Symp. Chem. Soc.* **1983**, *18*, 115.
(23) Richardson, R. K.; Ross-Murphy, S. B. *Int. J. Biol. Macromol.* **1987**, *9*, 257.
(24) Besio, G. J.; Leavesley, I. M.; Prud'homme, R. K.; Farinato, R. *J. App. Polym. Sci.* **1987**, *33*, 825.
(25) Morris, V. J.; Franklin, D.; l'Anson, K. *Carbohydr. Res.* **1983**, *121*, 13.
(26) Norton, I. T.; Goodall, D. M.; Fragou, S. A.; Morris, E. R.; Rees, D. A. *J. Mol. Biol.* **1984**, *175*, 371.
(27) Chow, A. W.; Fuller, G. G. *J. Rheol.* **1984**, *28*, 23.
(28) Rochefort, W. E. Ph.D. Thesis, University of California at San Diego, 1986.